REAL-TIME MEASUREMENTS OF PNA:DNA HYBRIDIZATION KINETICS WITH SILICON NANOWIRE BIOSENSORS

A. De, J. van Nieuwkasteele, E.T. Carlen*, and A. van den Berg*
BIOS Lab on a Chip Group, MESA+ Institute for Nanotechnology, University of Twente, THE NETHERLANDS

ABSTRACT

Real-time electronic detection of peptide nucleic acid (PNA):DNA hybridization is demonstrated with silicon nanowire (Si-NW) biosensors. A stable baseline platform is crucial for obtaining the Si-NW response for biosensing applications. An integrated Si-NW auto-sampler is demonstrated and used for kinetic molecular binding measurements. The equilibrium association constant is determined to be $K_A \approx 7\times10^6$ M^{-1} in 1 mM ionic strength buffer. The surface density of hybridized DNA is determined to be ~10^{12} molecules/cm^2 with a radiolabeled DNA-P^{32} assay. A 30× reduction in the measurement drift in Si-NW sensor response is obtained from 1.6 nA/hr to 0.04 nA/hr by using a differential measurement.

KEYWORDS

Nano-ISFET, silicon nanowire, PNA, hybridization kinetics

INTRODUCTION

The measurement of binding affinity of biomolecular complexes is important for molecular diagnostics and drug discovery, and label-free biosensors are emerging for high-throughput sample processing. Silicon nanowire (Si-NW) biosensors have the potential for massive parallelization with low per-sample costs. There are many challenges to estimate the binding affinity using real-time Si-NW measurements as the sensor surface area is small, which limits the sample concentrations to a few nM for analysis times on the order of 15 minutes due to limited molecular transport [1]. The Si-NW sensors are also sensitive to sample flow rate changes due to variations in streaming potential at the gate-oxide surface in low ionic strength buffers during sample switching that can introduce erroneous sensor responses [2].

We present an integrated Si-NW platform with automated sample injection into a microfluidic flow-cell and simultaneous electronic measurement thus ensuring stable sensor signals over the entire measurement cycle. The sample flow rate in the microfluidic flow cell is compatible with reaction-limited hybridization kinetics and a conventional Langmuir model is used to model the PNA:DNA complex formation.

EXPERIMENTAL

Surface functionalization

The p-type Si-NW sensors have been fabricated using plane dependent etching of silicon and reported previously by our group [3]. Uncharged thiolated PNA (Cys-TGT-ACA-TCA-CAA-CTA-NH_2) probe molecules are attached to the gate-oxide of the Si-NW sensors with a 3-amino propyl triethoxy silane (APTES) monolayer and hetero-bifunctional crosslinker sulfo succinimidyl cyclohexane carboxylate maleimide (sulfo-SMCC) to conjugate the aminated ends of the APTES layer to the thiolated PNA, as shown in Figure 1.

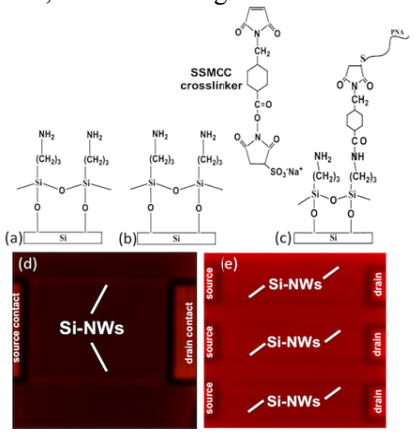

Figure 1: Surface functionalization steps of PNA on SiO_2 starting with (a) APTES, (b) maleimide activation on APTES layer with sulfo-SMCC, and (c) coupling of thiolated PNA to maleimide terminated APTES layer on SiO_2 (d) control Si-NW surface without crosslinker sulfo-SMCC, (e) Si-NW surface functionalized with PNA-Cy5.

Microfluidic integrated biosensing platform

The Si-NW chip functionalized with PNA probe is clamped with a microfluidic flow channel made from poly-dimethylsiloxane (PDMS). A platinum pseudo-reference electrode is inserted directly into the microchannel and used as a liquid front gate. The depletion mode p-type Si-NW sensors respond with increasing device current upon increases in negative gate potential due to the molecular binding of electronic charge. A Chemport Nanovolume injector valve is used

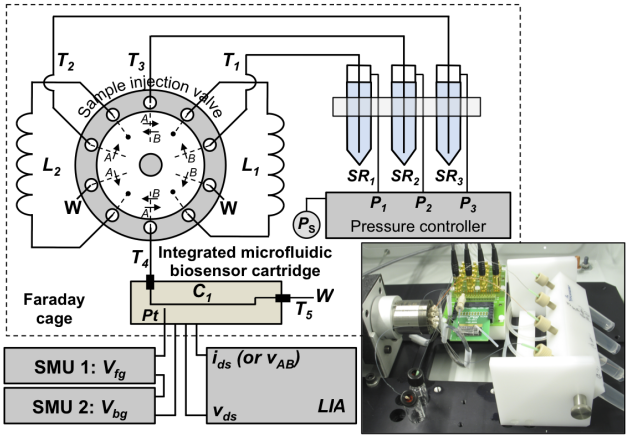

Figure 2: Schematic diagram of Si-NW integrated set up. (Lower right inset: image of integrated auto-sampler system.)

with a pressurized flow system, and sample loops in a balanced fluidic resistance circuit enabling analyte transport in the reaction-limited regime [1]. Si-NW microfluidic assembly is mounted with the injector valve auto-sampler flow system and simultaneous fluid and electrical measurement performed inside a Faraday cage as represented by the dotted border in Figure 2. A schematic diagram of the integrated Si-NW microfluidic and electrical set up is shown in Figure 2.

Electronic measurement

The device operation is controlled with DC voltage sources V_{fg} and V_{bg} (2400 SMU, Keithley). The platinum wire reference electrode provides the front-gate bias in solution. The Si-NW is driven with an AC (30 Hz) modulation voltage v_{ds} and the AC device current is converted to a voltage with a transconductance amplifier (TA) of a lock-in amplifier (LIA) (SR 830, Stanford Research Systems).

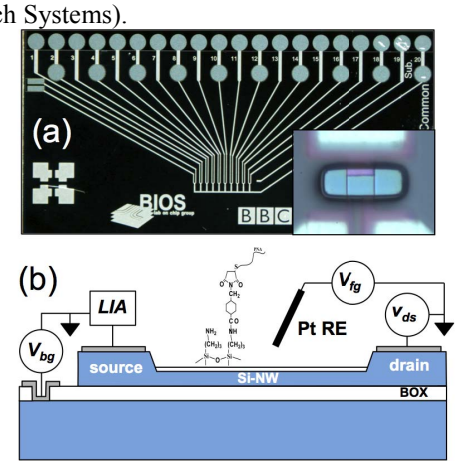

Figure 3: Si-NW measurement scheme. (a) Si-NW chip with inset showing optical image of 2-wire Si-NW device used for measurement (b) Si-NW measurement circuit for PNA:DNA hybridization detection.

For single sensor measurements the internal TA of the LIA is used (Figure 4a). For differential measurements, two external TA (SIM918, Stanford Research Systems) convert the currents into voltages v_A and v_B, respectively. The LIA measurement is then in differential mode (v_A-v_B) (Figure 4b). All biasing and measurement instruments are controlled using a custom-made Labview program.

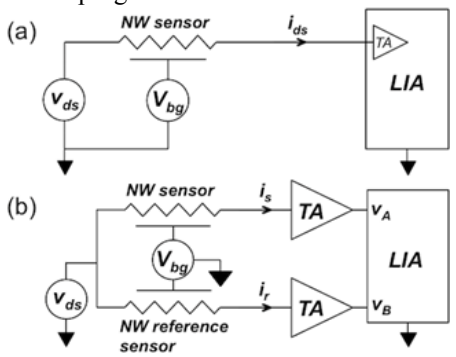

Figure 4: Electrical measurement configurations. (a) Single-device measurement circuit schematic. (b) Differential measurement circuit.

Probe surface density

The PNA probe surface coverage is important for the transduction of DNA hybridized to the Si-NW surface; a large probe surface density generates a large surface potential, however, a surface probe density too large can hinder the hybridization efficiency. Therefore, we have characterized the PNA probe surface density using both fluorescence and radioactive labeled assays. Target DNA (5'-TAG-TTG-TGA-TGT-ACA-3') was radiolabeled with γ-ATP^{32} and poly-nucleotide kinase following New England Biolabs protocol. Radiolabeled DNA-P^{32} was used to determine the hybridization density to two types of PNA in 1 mM, 23 mM, 137 mM NaCl concentration buffers, respectively. Normal PNA (Cys-TGT-ACA-TCA-CAA-CTA-NH_2) immobilized at its N-end and γ-PNA (Ac-TGT*(C6-SH)-ACA-TC*(C6-SH)A-CAA-C*(C6-SH)TA) immobilized along its backbone.

RESULTS AND DISCUSSION

Sample switching and flow rate effects

Measurements with Si-NWs for biosensing applications are commonly reported with very dilute ionic strength buffers since the Debye length is larger in low ionic strength buffer [4]. However, the effect of flow variation in low ionic strength buffers is very high due to the streaming potential of ions [2,5]. The streaming potential effect is greater in a low ionic strength buffer and reduces as the ionic strength increases beyond about 10 mM NaCl. We have characterized our Si-NW sensors by flowing 1 mM NaCl buffer at different flow rates.

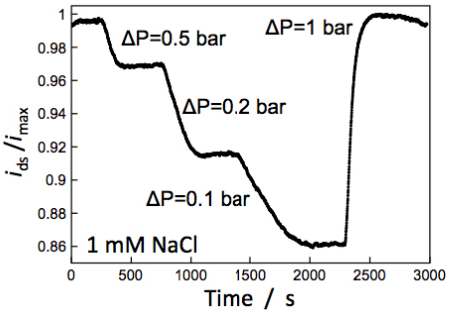

Figure 5: Measured Si-NW sensor current dependence on flow rate changes in a microfluidic channel. Pressure driven sample flow with 1 mM NaCl buffer for channel pressure changed from ΔP=1 bar to ΔP=0.5 bar to ΔP=0.2 bar and to ΔP=0.1 bar and then back to ΔP=1 bar.

Figure 5 shows an example of Si-NW sensor response to changes in the flow rate in the integrated microfluidic flow-cell where about 14% change in current response as the driving pressure across the microchannel is switched from ΔP=1 bar to ΔP= 0.1 bar. These results are consistent with previous reports, i.e. decreases in the flow rate result in a decrease in conductance of p-type Si-NW devices and increased ionic strength reduces the effect of conductance changes from sample flow rate changes [2].

Figure 6 shows that flow rate changes due to sample switching can be eliminated with the automated multi-sample injection system and pressure driven flow. The

Nanovolume sample injection valve, with its small internal dead volume, combined with pressure driven sample transport across balanced hydraulic resistances provides stable and rapid sample switching for biosensing experiments.

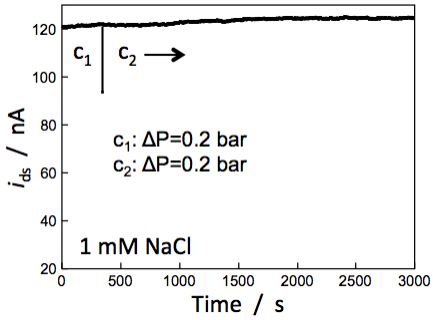

Figure 6: Injector switching of 1 mM NaCl buffer from position c_1 (ΔP=0.2 bar) to position c_2 (ΔP=0.2 bar) with the auto-sampler integrated biosensor platform.

PNA probe surface density

Radiolabeled DNA-P^{32} is used to estimate the DNA hybridization and it is determined that the PNA:DNA duplex surface density $N_s \sim 10^{12}$ molecules/cm^2. This hybridization density is with both normal vertically tethered PNA as well as horizontally tethered PNA (γ-PNA) probes [6]. The γ-PNA probe has significantly less non-specific binding of non-complementary DNA (NC DNA) as can be seen in Figure 7. The quantified hybridization densities shown in Figure 7 are tabulated in Table 1.

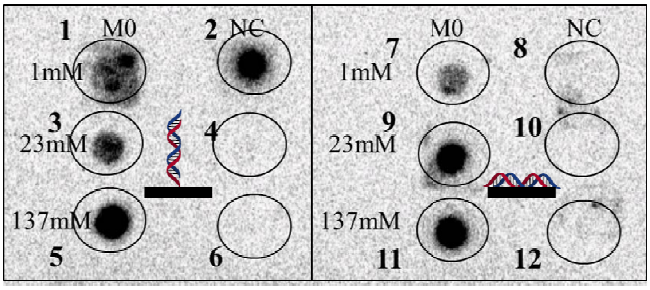

Figure 7: Complementary DNA (M0) and non-complementary DNA (NC) hybridized to surface attached PNA on SiO_2 surface. Left (1-6): vertical PNA:DNA hybridization. Right (7-12): horizontal γ-PNA:DNA hybridization. All experiments performed for 1 hour.

Table 1: DNA-P^{32} hybridization density from Figure 8.

No.	Surface density $\times 10^{12}$ mol/cm^2	No.	Surface density $\times 10^{12}$ mol/cm^2
1	1	7	0.5
2	11	8	0.01
3	0.5	9	2
4	0.02	10	0.05
5	2	11	2
6	0.05	12	0.1

DNA hybridization detection

The Si-NW integrated microfluidic set up is used for DNA hybridization detection. Briefly prior to hybridization measurement, a transconductance plot $g_m \approx (\Delta i_{ds})/(\Delta V_{fg})$ for the device being used is obtained by an increasing negative front gate scan at a fixed bias V_{bg} and v_{ds}, respectively. Figure 8 is a transconductance plot for the hybridization measurements. This determines the device sensitivity, and is used to convert the changes in i_{ds} due to pH or DNA hybridization to surface potential changes on the gate surface of the Si-NW. We have evaluated the hybridization affinity of 15-mer DNA to vertical standing complementary PNA probe molecules, covalently tethered to the gate-oxide of a two-wire Si-NW biosensor (Figure 3, inset), to be $K_A \approx 7\times10^6$ M^{-1} in 1 mM ionic strength, which is lower than a previous report [6].

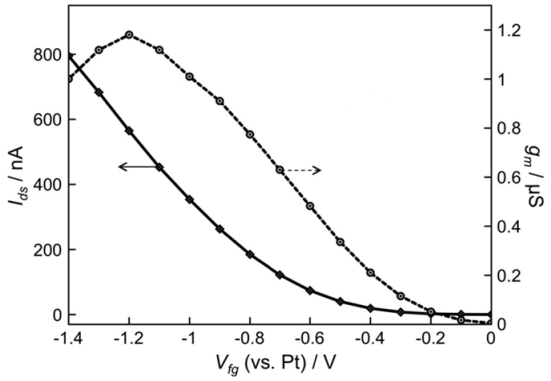

Figure 8: Si-NW front-gate biasing characteristics with platinum reference electrode.

However, affinity measurements of DNA:DNA hybridization using Si-NW sensors with electrostatically adsorbed probes in a 165 mM ionic strength buffer are similar to our measurements [7]. The surface potential change of the gate oxide upon hybridization of the DNA can be estimated with $\Delta\psi_o \approx (2kTq^{-1})(\sinh^{-1}((\sigma_{DNA}-\sigma_{ox})/\beta) - \sinh^{-1}(\sigma_{ox}/\beta))$, where ε_w=80 and c_o=1 mM, and $\sigma_{DNA} \approx N_s \times 15 \times q \times 10^4$ C/m^2 [8]. Since the density of PNA:DNA duplexes formed on the gate oxide surfaces in equilibrium is $N_s \sim 10^{12}$ duplexes/cm^2, which was measured using a P^{32} radioactive assay and is shown in Figure 7 and Table 1, we estimate an upper limit of $\Delta\psi_o \sim 10$ mV is estimated using an oxide charge density $\sigma_{ox} \approx 0.2$ C/m^2 for a *pH* 7 buffer [8].

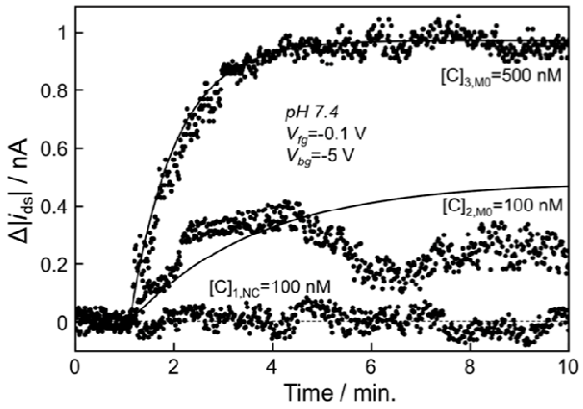

Figure 9: PNA:DNA duplex hybridization detection with $[C]_{3,M0}$=500 nM, $[C]_{2,M0}$=100 nM and $[C]_{1,NC}$=100 nM target concentrations and sample flow speed $v_s \sim 0.6$ mm/s.

The estimated surface potential changes correspond

to larger conductance changes compared to the measured conductance changes. From separate radioactive DNA-P^{32} assays it was discovered that a considerable amount of non-specifically adsorbed PNA on the surrounding polyimide insulation layer was present.

Differential measurement

The differential measurement setup is shown in Figure 4b. It is well known that the output response of ion sensitive field-effect transistor sensors, the microscale predecessors to Si-NW sensors, suffer from drift due to ion migration at the gate-oxide interface [9]. The drift measured from a two-wire Si-NW device is 1.6 nA/hr and that from a single split-contact Si-NW sensor pair in differential mode is 0.04 nA/hr and plotted in Figure 10. The drift has been reduced by a factor of 30× in case of differential mode. The quiescent output signal in this case is nulled to zero and so higher sensitivity in the sensor signal is detected due to reduced detection range of the instrument.

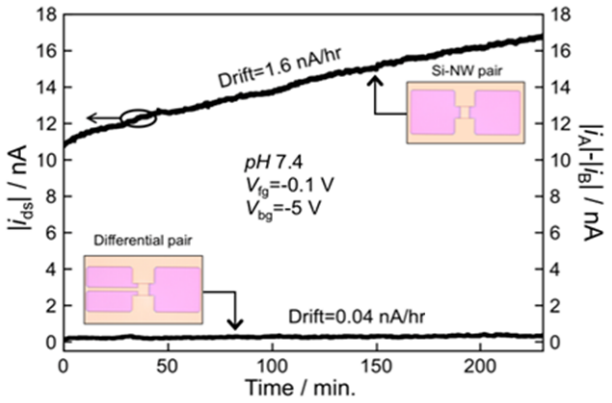

Figure 10: Differential Si-NW sensors and pair of Si-NW drift measurements.

CONCLUSION

We have been able to demonstrate a stable base-line measurement set up for Si-NW biosensing measurements, which eliminates erroneous noise due to low ionic strength buffers. The fluid delivery in the integrated Si-NW platform is at a high flow speed for analyte transport to be in the reaction-limited regime. The integrated Si-NW auto-sampler system has been used to study real-time kinetic parameter estimation of electronic PNA:DNA hybridization detection. The extracted equilibrium association constant $K_A \approx 7\times10^6$ M^{-1}, which is lower than previously reported values and the discrepancy, is attributed to analyte depletion effects, due to large amount of non-specific binding of PNA probes confirmed by radiolabed DNA hybridization. An improvement in the measurement of Si-NW response is made by introducing a differential measurement method, which effectively cancels out the inherent drift in Si-NW response by a factor of 30×. Further improvements to the electronic assay detection are being worked upon by including horizontally aligned PNA probes hybridization combined with differential sensor-reference Si-NW sensors.

REFERENCES

[1] T.M. Squires, R.J. Messinger, and S.R. Manalis,"Making it stick: Convection, reaction and diffusion in surface-based biosensors", *Nat. Biotechnol.*, vol. 26, pp. 417-426, 2008.

[2] D.R. Kim, C.H. Lee, and X. Zheng, "Probing flow velocity with silicon nanowire sensors", *Nano Lett.*, vol. 9, pp. 1984-1988, 2009.

[3] S. Chen, J.G. Bomer, E.T. Carlen, and A. Van den Berg, "Al_2O_3/silicon nanoISFET with near ideal Nernstian response", *Nano Lett.*, vol. 11, pp. 2334-2341, 2011.

[4] E. Stern, R. Wagner, F.J. Sigworth, R. Breaker, T.M. Fahmy, and M.A. Reed, "Importance of the debye screening length on nanowire field effect transistor sensors", *Nano Lett.*, vol. 7, pp. 3405-3409, 2007.

[5] R.B. Schoch, J. Han, and P. Renaud, "Transport phenomena in nanofluidics", *Rev. Mod. Phys.*, vol. 80, pp. 839-883, 2008.

[6] H. Park, A. Gemini, S. Sforza, R. Corradini, R. Marchelli, and W. Knoll, "Effect of ionic strength on PNA-DNA hybridization on surfaces and in solution", *Biointerphases*, vol. 2, pp. 80-88, 2007.

[7] Y.L. Bunimovich, Y.S. Shin, W.S. Yeo, M. Amori, G. Kwong, and J.R. Heath, "Quantitative real-time measurements of DNA hybridization with alkylated nonoxidized silicon nanowires in electrolyte solution", *J. Am. Chem. Soc.*, vol. 128, pp. 16323-16331, 2006.

[8] J. Fritz, E.B. Cooper, S. Gaudet, P.K. Sorger, and S.R. Manalis, "Electronic detection of DNA by its intrinsic molecular charge", *P. Natl. Acad. Sci. USA*, vol. 99, pp. 14142-14146, 2002.

[9] P. Bergveld, "The operation of an ISFET as an electronic device", *Sensor Actuator*, vol. 1, pp. 17-29, 1981.

CONTACT

*Arpita De; Tel: +31-534893107; a.de@utwente.nl

*E.T. Carlen; Tel: +31-534895399; e.t.carlen@utwente.nl